PB 181592
Price $1.25

UNITED STATES
DEPARTMENT OF THE INTERIOR

SALT CONCENTRATION AT PHASE BOUNDARIES IN DESALINATION PROCESSES

BY
MASSACHUSETTS INSTITUTE OF TECHNOLOGY
CAMBRIDGE, MASSACHUSETTS

OFFICE OF SALINE WATER

RESEARCH AND DEVELOPMENT PROGRESS REPORT NO. 95

For sale by the U.S. Department of Commerce, Office of Technical Services,
Washington, D.C., 20230

Created in 1849, the Department of the Interior--America's Department of Natural Resources--is concerned with the management, conservation, and development of the Nation's water, wildlife, mineral, forest, and park and recreational resources. It also has major responsibilities for Indian and Territorial affairs.

As the Nation's principal conservation agency, the Department of the Interior works to assure that nonrenewable resources are developed and used wisely, that park and recreational resources are conserved for the future, and that renewable resources make their full contribution to the progress, prosperity, and security of the United States--now and in the future.

U N I T E D S T A T E S

D E P A R T M E N T O F T H E I N T E R I O R

Stewart L. Udall, Secretary

Kenneth Holum, Assistant Secretary
for Water and Power Development

RESEARCH AND DEVELOPMENT PROGRESS REPORT NO. 95

SALT CONCENTRATION AT PHASE BOUNDARIES IN DESALINATION PROCESSES

by

T. K. Sherwood, P. L. T. Brian, and R. E. Fisher

MASSACHUSETTS INSTITUTE OF TECHNOLOGY

CAMBRIDGE, MASSACHUSETTS

for

OFFICE OF SALINE WATER

Charles F. MacGowan, Director

W. Sherman Gillam, Chief, Division of Research

Sidney Johnson, Chief, Branch of Physics
and Surface Chemistry

March 1964

Foreword

This is the ninety-fifth of a series of reports designed to present accounts of progress in saline water conversion with the expectation that the exchange of such data will contribute to the long-range development of economical processes applicable to large-scale, low-cost demineralization of sea or other saline water.

Except for minor editing, the data herein are as contained in the reports submitted by the Massachusetts Institute of Technology, under Contract No. 14-01-0001-295, covering research carried out through August 1963. The data and conclusions given in this report are essentially those of the Contractor and are not necessarily endorsed by the Department of the Interior.

Summary

Several desalination processes are based on water removal from a brine by transport of water, but not salt, across a phase boundary. Water being transported to the interface carries salt with it, and since the salt is not removed, the salt concentration in the solution in contact with the interface tends to be maintained at a higher value than in the bulk brine. The salt concentration gradient so established permits the diffusion of salt away from the interface as fast as it arrives. The result is that the process must operate to desalinate a brine having a higher salt concentration than that of the bulk saline solution.

This effect is not important in distillation, since the boiling solution is violently agitated. It can be serious, however, in water removal by freezing, solvent extraction, or reverse osmosis. Salt build-up at the surface of an osmotic membrane causes the effective osmotic pressure to be greater than the osmotic pressure of the bulk brine. The operating total pressure must be increased by approximately this increment to maintain the desired water withdrawal flux. Salt build-up may also result in the precipitation, on the membrane surface, of a relatively insoluble constituent of the brine.

The existing theories of diffusion and mass transfer permit the importance of salt build-up to be estimated. This report provides such estimates for both turbulent and laminar flow of brine

past the surface of an osmotic membrane. Both analyses suggest that the salt build-up phenomenon can be a serious obstacle to the development of reverse osmosis desalination processes.

With brine in turbulent flow at 1.0 ft per second through a 1.0-in. tube the ratio c_w/c_o is 1.30 at a water flux of 10 gallons per day per square foot of membrane, and 2.9 at 40 gallons per day per square foot. c_w and c_o represent the salt concentrations at the phase boundary and in the bulk brine, respectively.

The case of flow in a two-dimensional duct (as in a "stack" of osmotic membranes) is analyzed rigorously for the case of constant water flux. This analysis develops the relations expressing the salt concentration as a function of membrane spacing, duct length, and brine flow velocity, for all positions in the channel. The procedure is to combine the equations for salt diffusion with the velocity field developed by Berman for this case.

The numerical examples show that the salt build-up may not be serious for high brine velocities in very short ducts, providing the water removal rates are modest. At a water flux of 40 gallons per day per square foot, however, the salt concentration at the membrane surface may be several times that of the brine feed in the case of brine flowing at 1.0 ft. per second through a duct 0.1 in. wide and 25 in. long. Such an effect would mean a very substantial increase in the required total

pressure, since the osmotic pressure, which is some 380 psia for sea water, would be effectively increased nearly in proportion to c_w/c_o.

The analysis presented pertains to any constituent of the brine, and may be employed to describe the conditions which will lead to salt (e.g. calcium sulfate) precipitation on the membrane, as well as the increase in effective osmotic pressure due to total salt build-up

Salt build-up at the surface of membranes employed for reverse osmosis is evidently a serious matter even with the modest water fluxes attainable with present-day membranes. As better membranes are developed, permitting appreciably greater water production rates, the salt build-up phenomenon will become increasingly important.

Salt Concentration at Phase Boundaries in Desalination Processes

1. Introduction

The recovery of fresh water from salt solutions by freezing, reverse osmosis (ultrafiltration), or solvent extraction involves the removal of water from a brine by transport across a phase boundary. As ice forms, water passes from an aqueous solution across a liquid-solid phase boundary to the solid phase. In reverse osmosis, essentially pure water crosses the phase boundary from liquid to the solid osmotic membrane. In solvent extraction water is transported across a liquid-liquid interface.

In each case the bulk flow to the phase boundary tends to transport salt, with the result that the salt concentration at the interface is established at a higher level than in the main liquid bulk. Since the salt does not cross the interface, it must diffuse back into the liquid, and a salt concentration gradient is set up near the phase boundary. If water is withdrawn at a constant rate, the transport of salt towards the interface must be equal to the diffusion flux in the opposite direction, and the salt concentration gradient does not change with time.

Salt build-up at an ice surface reduces the freezing point below that of the bulk solution and requires that lower refrigerant temperatures be used. Salt build-up at the surface of an osmotic membrane increases the effective osmotic pressure which must be

overcome to accomplish water transport through the membrane. In both instances the higher salt concentration at the phase boundary results in higher desalination costs than would prevail if the surface could be maintained in contact with solution at the bulk brine concentration.

This report explores the theory of the salt build-up phenomenon in a preliminary way. Several simplifying assumptions will be made, since the purpose is to obtain only approximate estimates of the importance of the phenomenon described. The solid surface will be assumed to be smooth and in contact with salt solution moving parallel to the surface in either laminar or turbulent flow. A solution of a single salt will be treated, deferring until later the complications of diffusion in multiple-ion systems. The analysis will be restricted to isothermal systems, and the diffusion coefficient will be assumed to be independent of salt concentration. Free convection due to changes in liquid density is neglected, since this is presumed to be unimportant in most equipment of practical design.

2. Simple Film Theory

The film model pictures a thin stagnant liquid film of thickness y_1, adjacent to the interface. This presents the entire resistance to mass transfer between bulk liquid and solid surface. Figure 1 illustrates the concept.

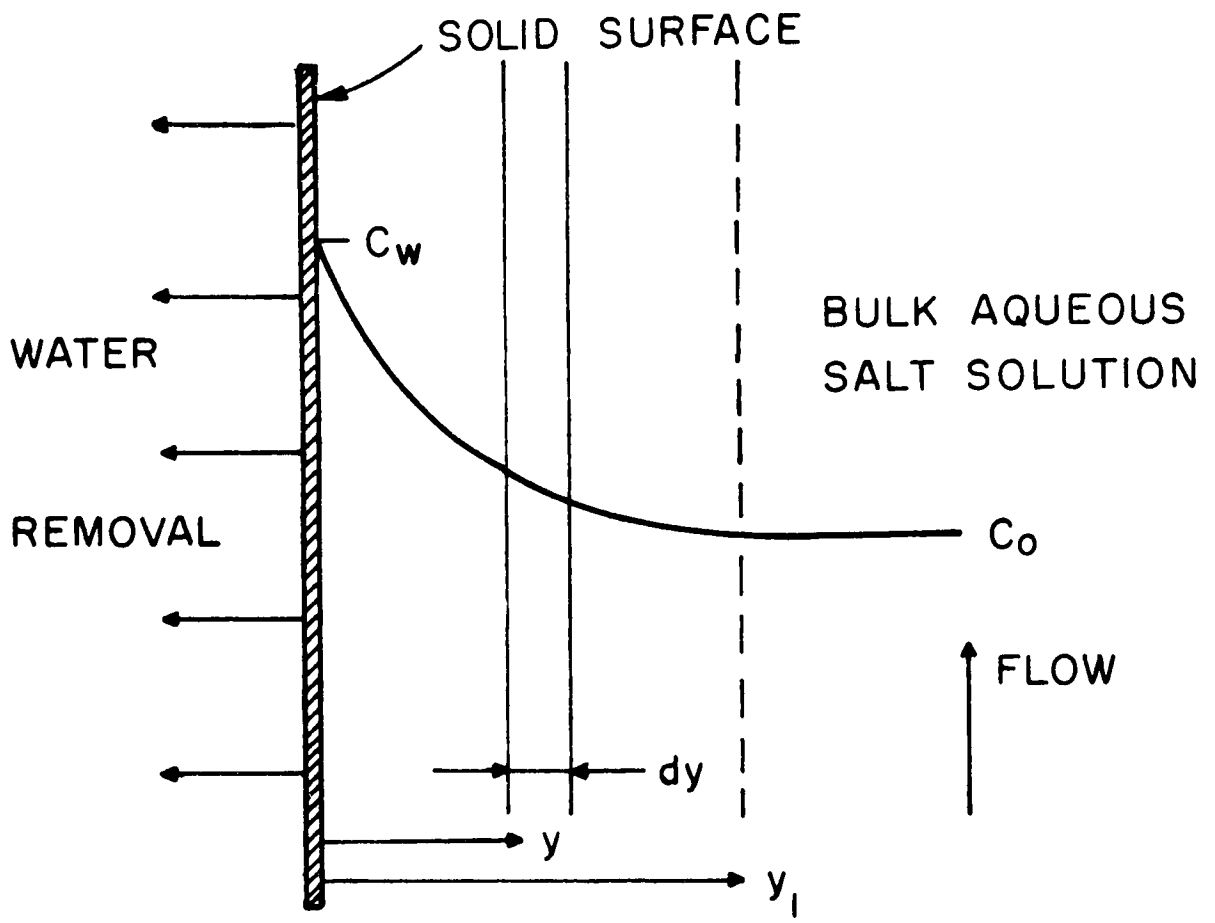

FIGURE I SIMPLE FILM MODEL

At steady state the salt concentration c will decrease with distance y in such a way that the salt diffusion flux away from the surface will be equal to the bulk transport of salt toward the surface due to water removal.

Let F represent the flux of water across the phase boundary, expressed as g moles/(sec)(sq cm total surface). Assume the water concentration (g moles/cm^3) to be independent of salt concentration over the range of salt concentrations of interest (for NaCl the variation at 25°C is only 0.2 percent over the range 0 to 10 weight percent salt). Then for the steady-state, the salt flux across the film is given by

$$F \frac{c}{c_L} + D_s \frac{dc}{dy} = 0 \quad (\text{g moles/sec cm}^2) \qquad (1)$$

where D_s is the diffusion coefficient of salt in the solution, and c_L is the water concentration. Integration leads to

$$\frac{c_w}{c_o} = \exp \left(\frac{Fy_1}{c_L D_s}\right) \qquad (2)$$

Data are available on mass transfer between solid surfaces and turbulent fluids for many geometric shapes and flow patterns in the form of mass transfer coefficients, k_s°, defined as the ratio of the diffusion flux to the overall concentration difference, solid surface to bulk fluid. For salt transfer, in the absence of water removal, the simple film theory model requires that k_s° be equal to D_s/y_1 and thus y_1 may be eliminated and Equation 2 may be written as

$$\frac{c_w}{c_o} = \exp \left(\frac{F}{c_L k_s^\circ}\right) \qquad (3)$$

where k_s°, the mass transfer coefficient to an impermeable wall (no water withdrawal), is assumed to be unaffected by the small water flux F found in freezing or reverse osmosis.

Data on mass transfer in many turbulent-flow systems have been correlated in terms of the Chilton-Colburn "j-factor" (11):

$$j_D \equiv \frac{k_s^\circ}{u_o} N_{Sc}^{2/3} = \text{function of } (N_{Re}) \qquad (4)$$

where N_{Sc} is the Schmidt number, ν/D_s, and N_{Re} is the Reynolds number for the flow of fluid past the surface at a bulk stream velocity u_o. To use existing correlations of experimental data, it is convenient to rewrite Equation 3:

$$\frac{c_w}{c_o} = \exp\left(\frac{F\, N_{Sc}^{2/3}}{c_L\, j_D\, u_o}\right) \qquad (5)$$

For steady turbulent flow in tubes and over flat surfaces the pressure drop required to overcome friction is almost entirely due to wall or "skin" friction. When this is true the mass-transfer j-factor, j_D, is found experimentally to be equal to f/2, where f is the friction factor in the Fanning equation (wall shear stress = $f\rho u_o^2/2$).

3. Turbulent Boundary Layer

Neither stagnant nor laminar layers of fluid are found at a surface in contact with a turbulent stream: mixing and eddy diffusion persist and disappear only in the limit as y approaches zero. Eddy diffusion is due to mixing, and transport by this mechanism is independent of molecular diffusivity. Assuming that molecular and eddy diffusion occur in parallel, the steady-state balance of salt fluxes becomes

$$F\,\frac{c}{c_L} + (D_s + \epsilon)\,\frac{dc}{dy} = 0 \qquad (6)$$

where ϵ represents a coefficient of eddy diffusion. (Thinking in terms of desalination, F has been defined as the water flux in the direction of decreasing y).

Various theories of mass transfer can be developed by integrating Equation 6, using some assumed relation between ϵ and the distance y. Several assumptions as to this relation have been successful in giving good agreement between calculated transfer coefficients and experimental data on both mass and heat transfer to turbulent flow. Two of these will be developed for application to the problem of mass transfer with water removal across the phase boundary.

Deissler. The Deissler (2) "analogy" is based on the semi-empirical relation:

$$\epsilon/\nu = n^2 u^+ y^+ \left[1 - \exp\left(-n^2 u^+ y^+\right)\right] \qquad (7)$$

in which n is an empirical constant, found by Deissler to be 0.124, and ν is the kinematic viscosity. The dimensionless quantities u^+ and y^+ are defined by

$$u^+ = \frac{u}{u_o}\sqrt{\frac{2}{f}} \qquad (8)$$

and

$$y^+ = \frac{u_o y}{\nu}\sqrt{\frac{f}{2}} \qquad (9)$$

Here u = velocity parallel to the surface at distance y

u_o = velocity of bulk fluid

f = friction factor in the Fanning equation.

Combining Equations 6, 7, 8, and 9:

$$\int_{c_w}^{c_o} \frac{dc}{c} = - \frac{F}{c_L u_o} \sqrt{\frac{2}{f}} \int_o^{\infty} \frac{dy^+}{\frac{1}{N_{Sc}} + n^2 u^+ y^+ \left[1 - \exp (n^2 u^+ y^+)\right]} \qquad (10)$$

where $N_{Sc} = \nu/D_s$.

At 25°C the kinematic viscosity of a 4 weight percent NaCl solution is approximately 0.0090 cm^2/sec, D_s is 1.61×10^{-5} cm^2/sec, and N_{Sc} is about 560. Molecular diffusion is important only very near the wall, where u^+ is essentially equal to y^+, and both are so small that Equation 10 may be simplified:

$$\ln \frac{c_w}{c_o} = \frac{F}{c_L u_o} \sqrt{\frac{2}{f}} \int_o^{\infty} \frac{dy^+}{\frac{1}{N_{Sc}} + (ny^+)^4} \qquad (11)$$

The upper limit of infinity is taken for convenience, since the integrand becomes negligible at values of y^+ corresponding to distances from the wall which are small compared with the dimensions of the flow channel.

The definite integral in Equation 11 is $\pi N_{Sc}^{3/4} / 2n\sqrt{2}$, whence, using a value of n of 0.124,

$$\frac{c_w}{c_o} = \exp \left(\frac{8.96 F N_{Sc}^{3/4}}{c_L u_o} \sqrt{\frac{2}{f}} \right) \qquad (12)$$

This is similar to Equation 3, with k_s° developed from Deissler's assumptions.

Vieth. Several of the better-known semi-theoretical "analogies" are reviewed in a 1959 article (12). Most suggest that k_s° should be proportional to $\sqrt{f}$, yet the experimental data suggest that k_s° is proportional to f. To obviate this difficulty, Ryan (13) has suggested that ϵ/ν be taken to be a function of y^{++} instead of y^+, where

$$y^{++} = \frac{u_o y f}{2\nu} = y^+ \sqrt{\frac{f}{2}} \tag{13}$$

Following this lead, Vieth et al (15) have proposed the relation

$$\epsilon/\nu = \beta' (y^{++})^3 \tag{14}$$

where β' is found to be 1.77.

This may be employed in the integration of Equation 6.

The development is similar to that based on Deissler.

Equation 11 becomes

$$\ln \frac{c_w}{c_o} = \frac{2F}{c_L u_o f} \int_o^\infty \frac{dy^{++}}{\frac{1}{N_{Sc}} + \beta' (y^{++})^3} \tag{15}$$

Evaluating the definite integral, this gives

$$\frac{c_w}{c_o} = \exp \left(\frac{4\pi F N_{Sc}}{3\sqrt{3}\,(\beta')^{1/3} c_w u_o f} \right)^{2/3}$$

$$= \exp \left(\frac{2 F N_{Sc}}{c_L u_o f} \right)^{2/3} \tag{16}$$

Since Vieth selected the value of 1.77 for β' in order that j_D would be equal to f/2, as called for by the Chilton-Colburn analogy, it is not unexpected that Equation 16 should reduce to Equation 5 when this equality holds.

Equations 10 and 16 are representative of the results obtainable from existing theories of mass transfer in turbulent flow, and it seems hardly worth while to pursue the development of the equations obtainable in the same way from the other well-known "analogies" between mass transfer and fluid friction.

Sample Calculations. The several theories provide a basis for estimating the magnitude of the effect of salt build-up at the surface of an osmotic membrane or at a growing ice surface, as encountered in the reverse-osmosis and freezing processes for desalination.

In order to visualize a definite case, the bulk solution will be taken to be 4 weight percent NaCl in water, and the following values assumed:

ν (kinematic viscosity) = 0.0090 cm^2/sec

d (inside diameter of pipe, or outside diameter of rotating cylinder) = 2.54 cm

N_{Sc} = 560

ρ (density of solution) = 1.025 g/cm^3

c_w = 0.0546 g moles water/cm^3 solution

Values of c_w/c_o have been calculated by the use of Equations 5 and 12, and the results plotted on Figures 2 and 3. Values of f for the round tube were obtained from Drew, Koo, and McAdams (3); j_D was taken as $\frac{f}{2}$, as suggested by the Colburn-Chilton correlation. For the rotating cylinder f was taken from the results of Theodorsen and Regier (14), and j_D from the correlation of data on dissolution of benzoic acid in water obtained by Eisenberg, Tobias, and Wilke (4). The case of the rotating cylinder is included because it is proposed to study this system experimentally in a continuation of the present investigation. The large values of c_w/c_o at low Reynolds numbers and high water fluxes have little quantitative significance, since solution properties were based on 4 weight percent salt.

The calculated results based on the Deissler theory are in approximate agreement with those for the simple film theory. For flow in a 1.0 in. i.d. tube at 1.0 ft/sec (u_o = 30.5, N_{Re} = 8600), c_w/c_o is 1.30 at a water flux of 10 gal/(day)(ft^2), but rises to 2.9 at 40 gal/(day)(ft^2). The fluxes reported by Loeb at U.C.L.A (7) are in the range of 10 to 20 gal/(day)(ft^2). At large water fluxes and low Reynolds numbers c_w/c_o becomes very large.

The value of k_s° for the salt solution flowing in a 1.0 in. tube at 1.0 ft/sec is approximately 0.00186 cm/sec. This corresponds to the diffusional resistance of a stagnant liquid

layer only 0.087 mm thick. Evidently a porous structure on top of the working membrane "skin" must be avoided, since this can greatly reduce k_s° and exaggerate the effect of salt build-up at the phase boundary.

Interpretation. The importance of these results becomes evident when c_w and c_o are converted to osmotic pressure. A 4 percent NaCl solution has an osmotic pressure of about 26 atmospheres (380 psia) at 25°C. If an applied pressure of 1000 psia is employed to accomplish reverse osmosis, the net pressure difference available to cause flow through the membrane would be 1000 - 380 = 620 psi if there were no salt build-up. If c_w/c_o is 1.3, the solution in contact with the membrane will contain 5.2 weight percent salt, and the effective osmotic pressure is approximately 510 psia. This corresponds to a reduction in the effective pressure difference from 620 to 490 psi, or 21 percent. Since the osmotic pressure is approximately proportional to salt concentration, the ratio c_w/c_o is roughly the factor by which the osmotic pressure is multiplied to obtain the effective osmotic pressure.

The best present osmotic membranes provide such low water fluxes that the fixed charges on the membrane stacks represent a large part of the cost of water produced by reverse osmosis. Better membranes will doubtless be developed, but the problem of salt build-up will become increasingly serious as water fluxes

increase. Figure 2 suggests that an improved membrane operated at 100 gal/(day)(ft^2) with a velocity of 1.0 ft/sec in a 1-in. tube would have to overcome an effective osmotic pressure corresponding to a salt concentration many times larger than that of the bulk brine. The difficulty might be partially overcome by operating at much higher velocities, but the pumping power required to circulate the solution would then be greatly increased.

The curves of Figures 2 and 3 may be used to estimate the importance of salt build-up at an ice surface in lowering the freezing point. Freezing rates of 0.10 to 10 mm/min (and even greater) have been reported. A rate of 0.1 mm/min corresponds to $F = 83 \times 10^{-6}$. Figure 2 indicates that c_w/c_o at this water flux and a bulk velocity of 1.0 ft/sec might be expected to be about 2.5. This would mean that the freezing point of the solution in contact with the ice surface (10 percent salt) would be -6.5°C, or 4.1°C lower than that of the bulk solution containing 4 weight percent salt. Brine trapped in dendrites at the growing ice surface will have a higher salt concentration than the bulk solution. The practical importance of these effects will evidently depend greatly on the rate of freezing and the nature of the freezing process.

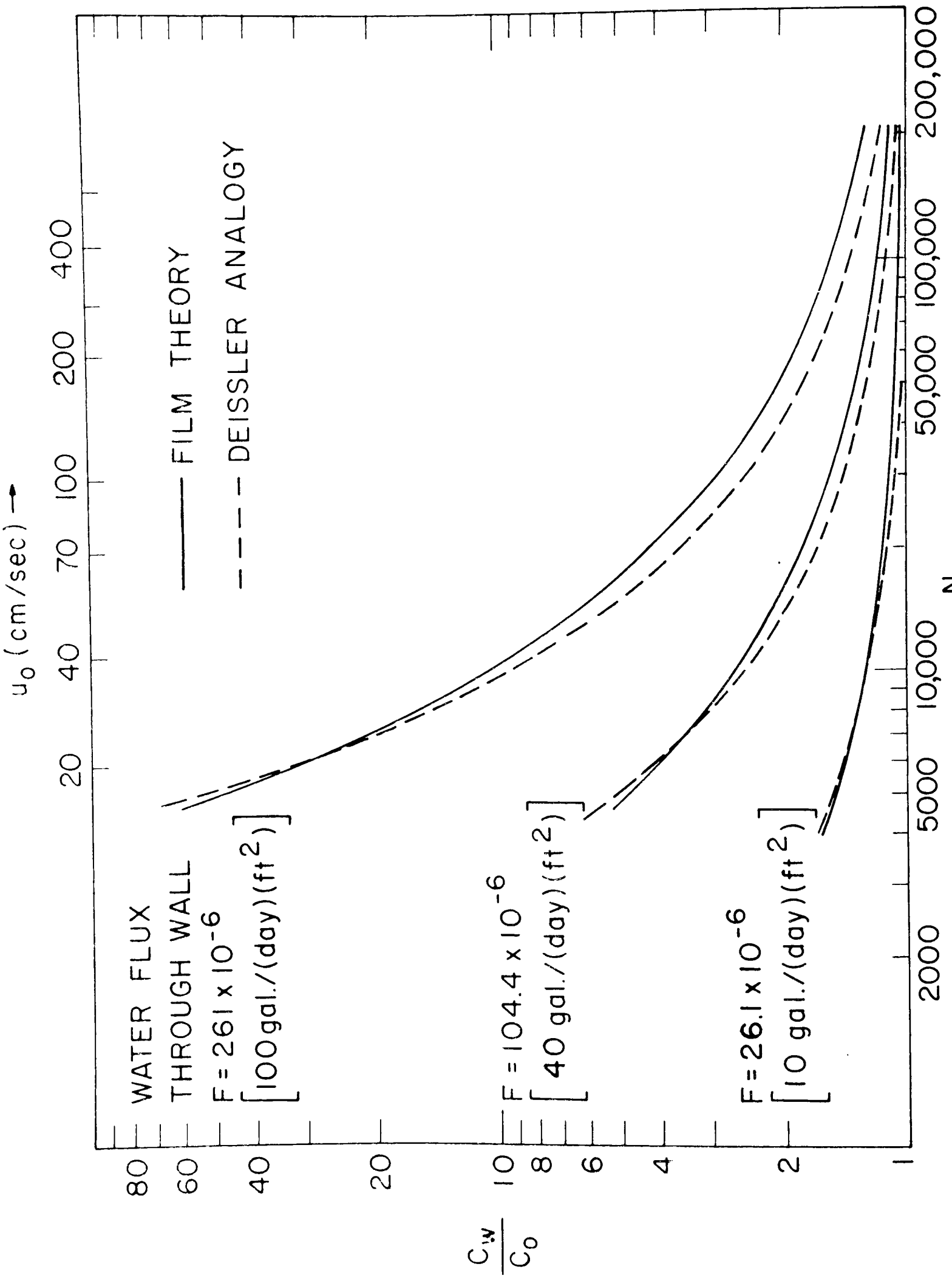

FIGURE 2 TURBULENT FLOW IN ROUND TUBE

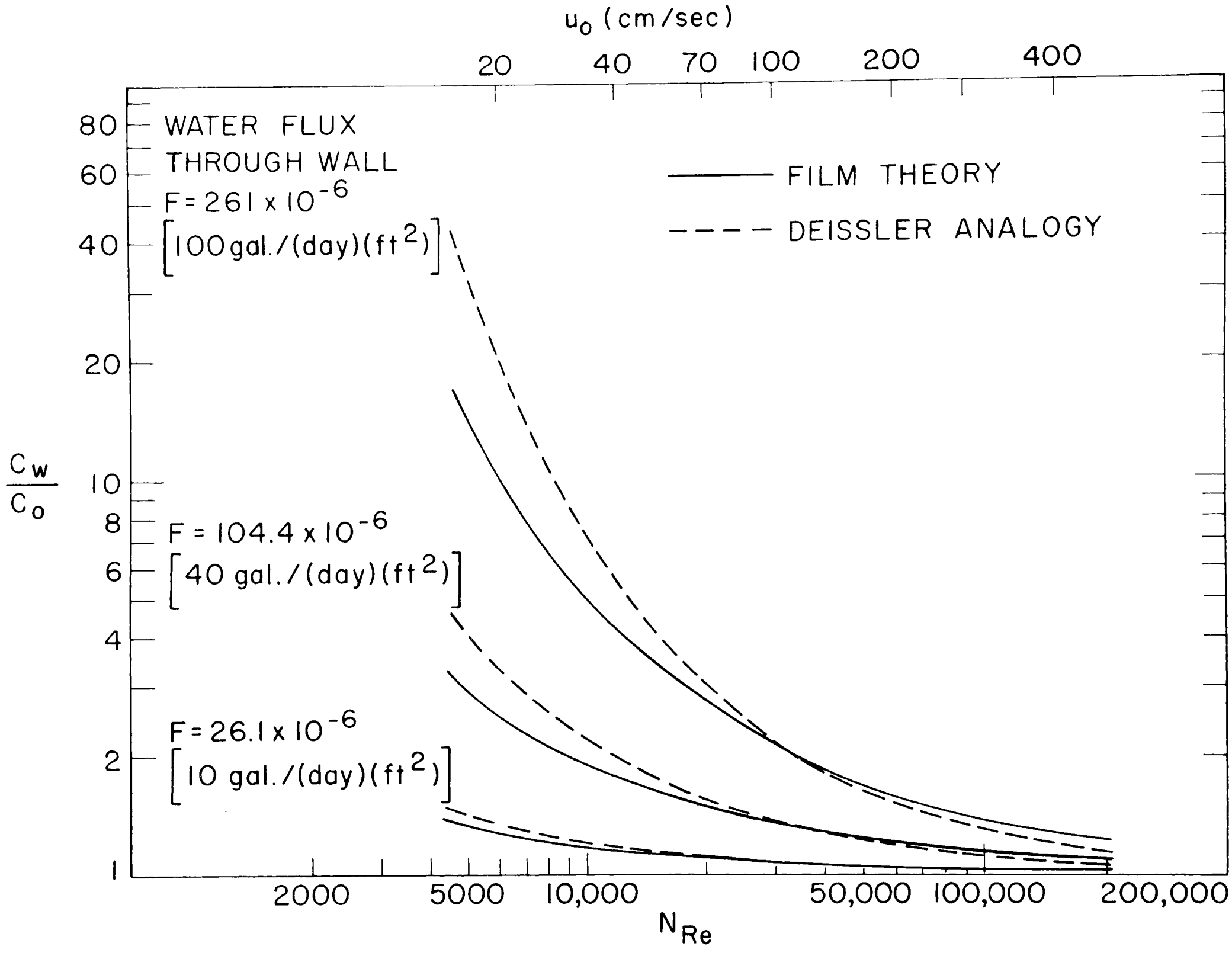

FIGURE 3 TURBULENT FLOW CYLINDER ROTATING IN BRINE

4. Laminar Flow

Practical equipment designs for reverse osmosis will probably not permit the use of the large flow passages and flow rates which result in turbulent flow. The least expensive membrane applications, for example, involve stacks of flat membranes separated by narrow passages for liquid flow, as used for electrodialysis. It is desirable, therefore, to develop the theory of salt build-up at the walls of narrow passages through which brine passes in laminar flow.

That the effect of salt build-up is important is well demonstrated by the recent results of Merten, Lonsdale, and Riley (9, 10), who found the water throughput to increase 30 to 45 percent as the brine velocity was raised from 5 to 40 cm/sec. These tests were run with laminar flow in a 0.1 in. passage over a flat membrane 3 inches long, using solutions containing 5.2 to 5.4 percent salt and applied pressures of 940 to 1540 psia. The effect of salt build-up was evidently substantial, though the water fluxes were quite low. The analogous mass transfer problem in electrodialysis has received much study in connection with stack design.

Within the limitations of certain reasonable assumptions, the path of all fluid elements is known for laminar flow. In principle, the problem is completely solvable. The mathematical analysis is difficult, however, since the flow pattern and salt

gradients change along the length of the passage, and the salt build-up effect varies with distance from the liquid supply point.

5. Laminar Flow in a Two-Dimensional Duct

An appealing design for reverse osmosis desalination cells is that of flat, parallel, semi-permeable walls separated by a narrow gap, i.e. a narrow rectangular duct. This design, where the distance between the walls is much smaller than the other dimensions, is essentially a two-dimensional configuration. For the axial flow rates of interest the flow regime will be laminar.

The concentration profiles are evaluated by considering the interaction of the velocity field with the mass transfer. The initial step in the analysis, i.e., the formulation of the two-dimensional laminar velocity field with porous walls, has been accomplished by Berman (1) for the case of an incompressible fluid with a constant rate of withdrawal through the walls. For the present analysis the latter restriction is inappropriate since as the concentration of salt at the wall increases the osmotic pressure increases and thus, the flux through the wall varies along the passage as the bulk salt concentration changes. The error introduced by this simplification will be discussed later in conjunction with the computer results.

Analysis

Consider the geometry of the system to be that illustrated i
Figure 4.

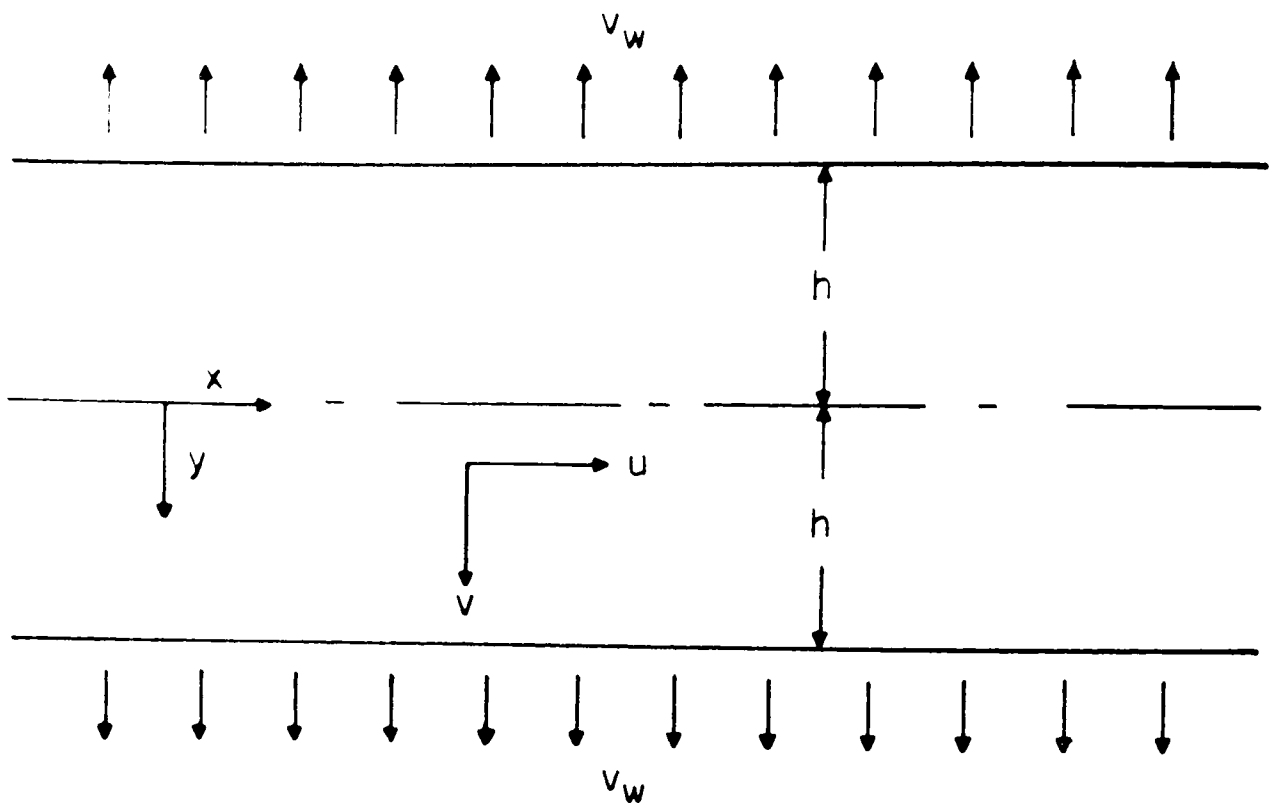

FIGURE 4

Assume:

1. incompressible, ideal fluid
2. fully developed laminar flow
3. constant withdrawal velocity, i.e. uniform flux of water through the walls.

The equation of continuity is

$$\frac{\partial u}{\partial x} + \frac{\partial v}{\partial y} = 0 \qquad (17)$$

The Navier-Stokes equations are:

for the x-direction

$$u \frac{\partial u}{\partial x} + v \frac{\partial u}{\partial y} = - \frac{1}{\rho} \frac{\partial p}{\partial x} + \nu \left(\frac{\partial^2 u}{\partial x^2} + \frac{\partial^2 u}{\partial y^2} \right) \tag{18}$$

for the y-direction

$$u \frac{\partial v}{\partial x} + v \frac{\partial v}{\partial y} = - \frac{1}{\rho} \frac{\partial p}{\partial y} + \nu \left(\frac{\partial^2 v}{\partial x^2} + \frac{\partial^2 v}{\partial y^2} \right) \tag{19}$$

The equation for the mass transfer of salt is

$$\frac{\partial}{\partial x} (u c) + \frac{\partial}{\partial y} (v c - D_s \frac{\partial c}{\partial y}) = 0 \tag{20}$$

The velocity field is symmetrical with respect to the mid-plane of the duct. The boundary conditions that describe the velocity field in the upper half of the duct are:

no slip at the wall

$$u (x, h) = 0 \tag{21}$$

constant rate of withdrawal

$$v (x, h) = v_w \quad \text{a constant} \tag{22}$$

symmetry

$$v (x, o) = 0 \tag{23}$$

$$\left. \frac{\partial u}{\partial y} \right)_{y=0} = 0 \tag{24}$$

The boundary conditions associated with the mass transfer equation are:

symmetry

$$\left.\frac{\partial c}{\partial y}\right|_{y=0} = 0 \tag{25}$$

initial concentration profile

$$c\ (o,\ y) = c_o \quad \text{a constant} \tag{26}$$

material balance on salt at the wall

$$v_w c\ (x,\ h) = D_s \left.\frac{\partial c}{\partial y}\right|_{y=h} \tag{27}$$

A flat initial concentration profile (Equation 26) is not a necessary restriction but was chosen for convenience to illustrate the decay of the concentration profile. The last boundary condition comes from a material balance on an infinitesimal control volume adjacent to the wall.

Velocity Field

The second and third assumptions listed above give rise to a major simplification of the velocity field. That is, the radial component of the velocity is independent of axial position. Equation 19 becomes

$$v\ \frac{\partial v}{\partial y} = -\frac{1}{\rho}\ \frac{\partial p}{\partial y} + \nu \frac{\partial^2 v}{\partial y^2} \tag{28}$$

The solution of the differential equations for the velocity field (Equations 17, 18, and 28), together with the associated boundary conditions (Equations 21, 22, 23, and 24) has been accomplished by Berman (1). He used a Reynolds number based on withdrawal velocity as a perturbation parameter to describe the deviations from Poiseuille flow. The solution given is

$$u\ (x,\ y) = \frac{3}{2}\left[\bar{u}(o) - \frac{v_w x}{h}\right]\left[1 - \left(\frac{Y}{h}\right)^2\right]\left\{1 - \frac{N_F}{420}\left[2\text{-}7\left(\frac{Y}{h}\right)^2 - 7\left(\frac{Y}{h}\right)^4\right]\right\} \tag{29}$$

and

$$v(y) = v_w\left\{\frac{Y}{2h}\left[3 - \left(\frac{Y}{h}\right)^2\right] - \frac{N_F}{280}\,\frac{Y}{h}\left[2 - 3\left(\frac{Y}{h}\right)^2 + \left(\frac{Y}{h}\right)^6\right]\right\} \tag{30}$$

where

$$N_F \equiv \frac{v_w h}{\nu} \tag{31}$$

The second-order term was small and was neglected. The above solution is valid only for a value of N_F not much greater than unity.

The velocity field equations can be further simplified for the present analysis by comparing the relative magnitude of the terms. The maximum value of the N_F used in the present study was about 0.02. It is apparent that for $N_F < 0.02$ the error introduced by writing

$$u(x, y) = \frac{3}{2}\left[\bar{u}(o) - \frac{v_w x}{h}\right]\left[1 - \left(\frac{y}{h}\right)^2\right] \tag{32}$$

and

$$v(y) = \frac{v_w y}{2h}\left[3 - \left(\frac{y}{h}\right)^2\right] \tag{33}$$

is less than 0.2%.

Concentration Field

With the initial step of formulating the velocity field accomplished, the next step is the formulation of the concentration field. A few definitions to be used are:

$$\left.\begin{aligned} L \equiv \frac{x}{h}, \quad R \equiv \frac{y}{h}, \quad U \equiv \frac{u}{\bar{u}(o)}, V \equiv \frac{v}{v_w} \\ C \equiv \frac{c}{c_o}, \quad \delta \equiv \frac{v_w}{\bar{u}(o)}, \quad \alpha \equiv D_s/v_w h \end{aligned}\right\} \tag{34}$$

The velocity field equations can be rewritten as

$$U(L, R) = \frac{3}{2}(1 - \delta L)(1 - R^2) \tag{35}$$

$$= f(L) \cdot g(R) \tag{36}$$

where

$$f(L) \equiv \frac{3}{2}(1 - \delta L) \tag{37}$$

$$g(R) \equiv (1 - R^2) \tag{38}$$

and

$$V(R) = \frac{1}{2} R (3 - R^2) \tag{39}$$

Equation 20 then becomes

$$\frac{\partial}{\partial L} (UC) + \delta \frac{\partial}{\partial R} (VC - \alpha \frac{\partial C}{\partial R}) = 0 \tag{40}$$

with the associated boundary conditions

$$C (o, R) = 1 \tag{41}$$

$$\frac{\partial C}{\partial R}\Bigg|_{R=0} = 0 \tag{42}$$

and

$$C (L, 1) = \alpha \frac{\partial C}{\partial R}\Bigg|_{R=1} \tag{43}$$

Assuming the solution to be of the forr

$$C(L, R) = X(L) \cdot Y(R) \tag{44}$$

and using a separation of the variables technique, Equation 40 becomes

$$-\frac{\frac{d}{dL}\left[f(L)\ X\right]}{\delta X} = \frac{\frac{d}{dR}\left[VY - \alpha Y'\right]}{g(R)\ Y} = \beta \tag{45}$$

The two ordinary differential equations that result are:

$$\frac{d}{dL}\left[f(L).\ X\right] = -\beta\ \delta X \tag{46}$$

$$\frac{d}{dR}\left[VY - \alpha Y'\right] = \beta\, g(R) \cdot Y \tag{47}$$

with the boundary conditions

$$Y'(o) = 0 \tag{48}$$

$$\alpha\, Y'(1) = Y(1) \tag{49}$$

The solution of the axial eigenfunction equation is immediately

$$X = \left[1 - \delta L\right]^{(\frac{2}{3}\beta - 1)} \tag{50}$$

The solution of the radial eigenfunction equation is not so simple. The analysis of the radial eigenfunctions will be presented in two parts: First showing that the solution exists and is complete, and finally obtaining the specific solution.

It is apparent from past experience that the concentration field must be described as an infinite series, i.e.

$$C\ (L,\ R) = \sum_{n=1}^{\infty} B_n\ X_n(L) \cdot Y_n(R) \tag{51}$$

or

$$C(L,\ R) = \sum_{n=1}^{\infty} B_n \left[1 - \delta L\right]^{(2/3\beta_n - 1)} Y_n(R) \tag{52}$$

where X_n and Y_n are taken to be the axial and radial eigenfunctions respectively, with the imposed boundary conditions. This means that

Equation 52 must

1. satisfy the partial differential equation for mass transfer,
2. satisfy the boundary conditions imposed by Equations 42 and 43, and
3. satisfy the initial concentration profile, Equation 41,

$$C(O,\ R) = 1 = \sum_{n=1}^{\infty} B_n\ Y_n(R)$$

i.e., if unity can be expanded in an infinite series of the radial eigenfunctions.

Condition (1) is satisfied by the separation of variables procedure, and condition (2) is met because the radial eigenfunctions will satisfy Equations 48 and 49. As background material for the third condition two preliminary integrations will be made. First the original partial differential equation is integrated to yield

$$\int_o^1 \frac{\partial}{\partial L}(UC)\,dR + \int_o^1 \delta \frac{\partial}{\partial R}\left(VC - \alpha \frac{\partial C}{\partial R}\right)dR = 0 \qquad (53)$$

or

$$\frac{\partial}{\partial L}\left[\int_o^1 UC\,dR\right] + \delta\left[VC - \alpha\ \frac{\partial C}{\partial R}\right]_o^1 = 0 \qquad (54)$$

The second term of Equation 54 vanishes at both limits, leaving

$$\frac{\partial}{\partial L}\left[\int_o^1 UC\,dR\right] = 0 \qquad (55)$$

At the inlet (x=o)

$$\int_o^1 U(O,\ R)\cdot C(O,\ R)\ dR \ = \ 1 \qquad (56)$$

and so

$$\int_o^1 U(L,\ R)\cdot C(L,\ R)\ dR \ = \ 1 \qquad (57)$$

or

$$\sum B_n X_n \int_o^1 (1 - R^2)\ Y_n\ dR \ = \ \frac{2}{3}\ (1 - \delta L)^{-1} \qquad (58)$$

Second the radial eigenfunction differential equation is integrated in a manner similar to that of the mass transfer equation, and the result is

$$\beta_n \int_o^1 (1 - R^2)\ \ Y_n\ dR \ = \ 0 \qquad (59)$$

For

$$\beta \neq 0$$

$$\int_o^1 (1 - R^2)\ \ Y_n\ dR \ = \ 0 \qquad (60)$$

but for $\beta = 0$,

$$\int_o^1 (1 - R^2)\ \ Y_n\ dR \ \neq \ 0 \qquad (61)$$

In order for Equation 59 to be consistent with equation 58, an eigenvalue must be zero, and this eigenvalue must correspond to a non-trivial eigenfunction solution. To verify these two points substitute $\beta = 0$ into the radial eigenfunction. Thus

Equation 47 becomes

$$\frac{d}{dR}\left[V\,Y_o - \alpha\,Y_o'\right] = 0 \tag{62}$$

and solving

$$Y_o = \exp\left\{\frac{1}{\alpha}\int V dR\right\} \tag{63}$$

or

$$Y_o = \exp\left\{\frac{R^2}{8\alpha}\,(6 - R^2)\right\} \tag{64}$$

Y_o can easily be shown to conform to the boundary conditions of Equations 48 and 49, thus allowing Equation 58 to be written

$$B_o = \frac{2/3}{\int_o^1 (1 - R^2)\,Y_o\,dR} \tag{65}$$

The coefficient of the first term in the expansion has been determined. Yet to be found is the general expression for the coefficients. For convenience to the following argument the radial eigenfunction differential equation is rewritten as.

$$\alpha\,Y_n'' - V\,Y'_n - V'Y_n + g(R)\,\beta_n\,Y_n = 0 \tag{66}$$

The Y_n functions are orthogonal with respect to a weighting function ϕ. Where ϕ is given by (6)

$$\phi = \frac{g(R)}{\alpha}\quad \Psi$$

and

$$\frac{\Psi'}{\Psi} = - \frac{V}{\alpha}$$

giving

$$\phi = \frac{q(R)}{\alpha} \exp \left\{ - \frac{1}{\alpha} \int V dR \right\} \tag{67}$$

or

$$\phi = \frac{1 - R^2}{\alpha} \left\{ \exp \frac{R^2}{8\alpha} (R^2 - 6) \right\} \tag{68}$$

so that

$$B_n = \frac{\int_o^1 \phi \, Y_n \, dR}{\int_o^1 \phi \, Y_n^{\,2} \, dR} \tag{69}$$

which agrees with Equation 65 when n = 0.

If in fact a function F(R), instead of unity, had been expanded, i.e.

$$F(R) = \sum K_N \, Y_N \, (R) \tag{70}$$

giving

$$\int_o^1 (1 - R^2) \, F(R) \, dR = K_o \int_o^1 Y_o \, (1 - R^2) \, dR \tag{71}$$

and also

$$K_o = \frac{\int_o^1 \phi \, F(R) \, Y_o \, dR}{\int_o^1 \phi \, Y_o^{\,2} \, dR} \tag{72}$$

then

$$\int_o^1 (1 - R^2) \, F(R) \, dR = \frac{\int_o^1 \phi \, F(R) \, Y_o \, dR}{\int_o^1 \phi \, Y_o^{\,2} \, dR}$$

$$X \int_0^1 (1 - R^2)\, Y_o \, dR \tag{73}$$

When F(R) = 1 both sides of the equation reduce to 2/3 and the solution is complete.

The final phase of the solution is to solve explicitly the radial eigenfunction. A convenient form of the radial eigenfunction differential equation is

$$Y_n'' - \frac{1}{2\alpha} R\,(3 - R^2)\, Y_n' - \frac{3 - 2\beta_n}{2\alpha} (1 - R^2)\, Y_n = 0 \tag{74}$$

Following the method of Frobenius (5), the solution becomes

$$Y_n = A_o + A_1 R + \ldots + A_j R^j + \ldots \tag{75}$$

where

$$A_2 = \frac{3 - 2\beta_n}{4\alpha} A_o$$

$$A_3 = \frac{6 - 2\beta_n}{12\alpha} A_1$$

$$A_4 = \frac{9 - 2\beta_n}{24\alpha} A_2 + \frac{2\beta_n - 3}{24\alpha} A_o \tag{76}$$

$$A_j = \frac{3(j - 1) - 2\beta_n}{2\alpha\, j(j - 1)} A_{j-2} + \frac{2\beta_n - (j-1)}{2\alpha\, j(j - 1)} A_{j-4}$$

By defining

$$f_{2j} \equiv \frac{A_{2j}}{A_o} \text{ , and } f_{2j-1} \equiv \frac{A_{2j-1}}{A_1}$$

Equation 75 becomes

$$Y_n = A_o \left\{1 + f_2(\beta_n)R^2 + ... + f_{2j}(\beta_n)R^{2j} + ...\right\}$$
$$+ A_1 \left\{R + f_3(\beta_n) + ... + f_{2j-1}(\beta_n)R^{2j-1} + ...\right\} \quad (77)$$

The boundary condition of Equation 48 demands that A_1 be identically zero. The final boundary condition gives the eigenvalue-determining equation as

$$1 = (2\alpha-1)f_2(\beta_n) + ... + (2j\alpha-1)\ f_{2j}(\beta_n) \quad (78)$$

The constant A_o appears in the final solution only as a product with the constants B_n. Thus A_o is conveniently chosen to be unity without loss of generality.

Method of Solution

The IBM 7090 digital computer was programmed to solve the relevant equations. The program consisted of two parts: The first part solved Equation 78 by trial and error for the eigenvalues; the second part employed the eigenvalues calculated to eight significant figures and calculated the concentration field. The integration of Equation 69 was accomplished numerically by Simpson's rule.

Results

Before discussing the computer results it is of interest to describe the far-downstream concentration profiles, i.e. where only the first term of Equation 52 remains. This is the term given by $\beta = 0$. Figure 5 shows how the ratio of the wall concentration to the centerline concentration varies with the withdrawal velocity parameter N_F. The results in Figure 5 show that the "far downstream" profile results in quite unfavorable values of c_w/c_L, and thus for commercially appealing flow rates the length of the flow channel should be short and narrow.

The right-hand side of the Equation 78 is plotted against β in Figure 6. The eigenvalues are those values of β at which the ordinate in Figure 6 is equal to unity. The eigenvalues depend only upon the value of α. The three values of α shown indicate that as α decreases, the eigenvalues become smaller.

Figure 7 shows how the ratio of the concentration at the wall to the feed concentration varies with the fraction of water removed. Also shown is the ratio of the concentration at the wall to the center line concentration, which approaches an asymptote as the fraction removed approaches 1.0. These results are replotted in Figure 8 to show the effect of the Reynolds number at three dimensionless distances. The constants of Equation 52 are tabulated in Table 1 of the appendix. Table 2 of the appendix presents the value of the radial eigenfunctions at 11 points in the duct.

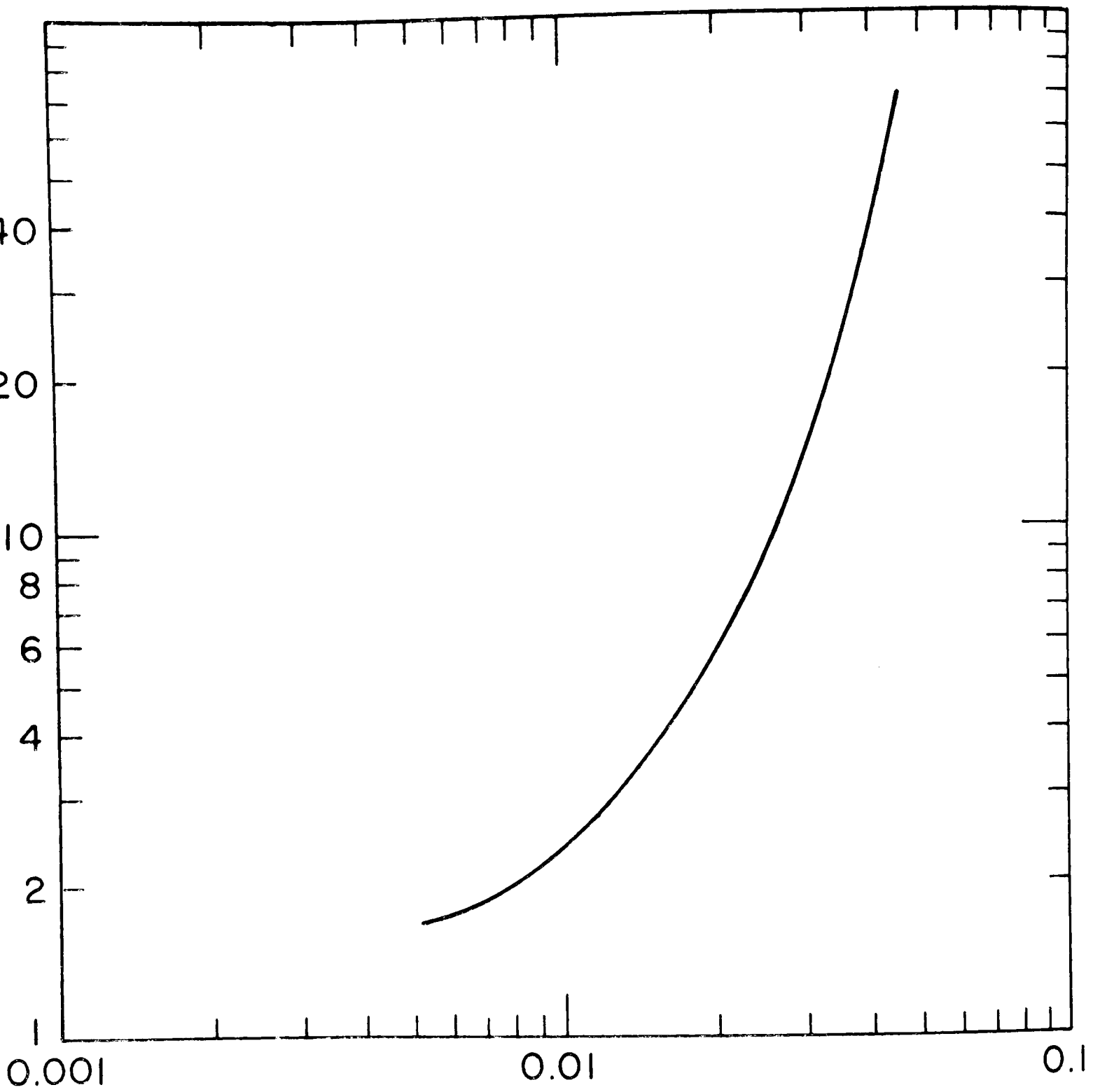

FIGURE 5 RATIO OF SALT CONCENTRATION AT WALL TO CONCENTRATION AT MIDPLANE "FAR DOWNSTREAM" FROM INLET

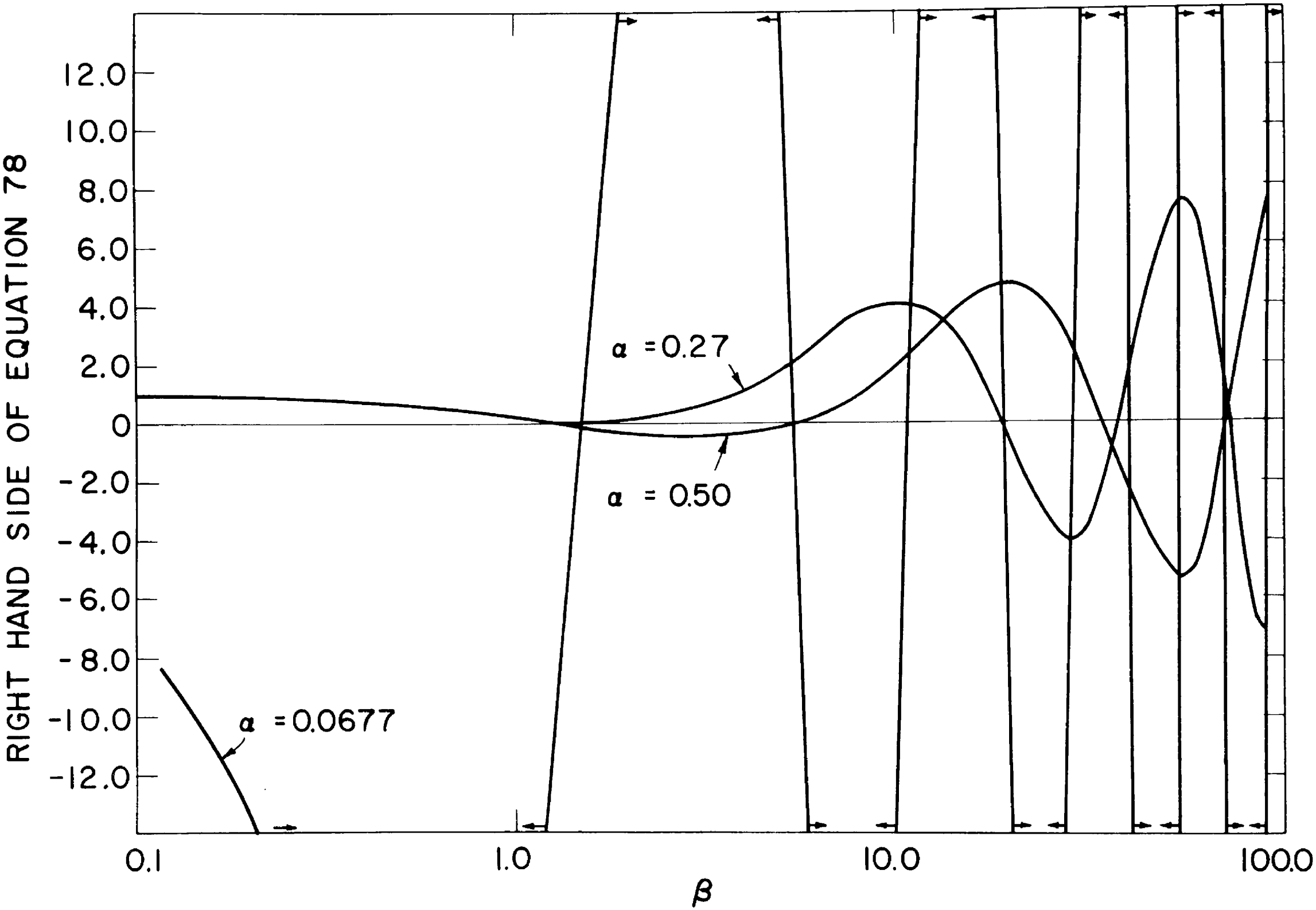

FIGURE 6 VALUES OF THE RIGHT-HAND SIDE OF EQUATION 78 PLOTTED VS. β

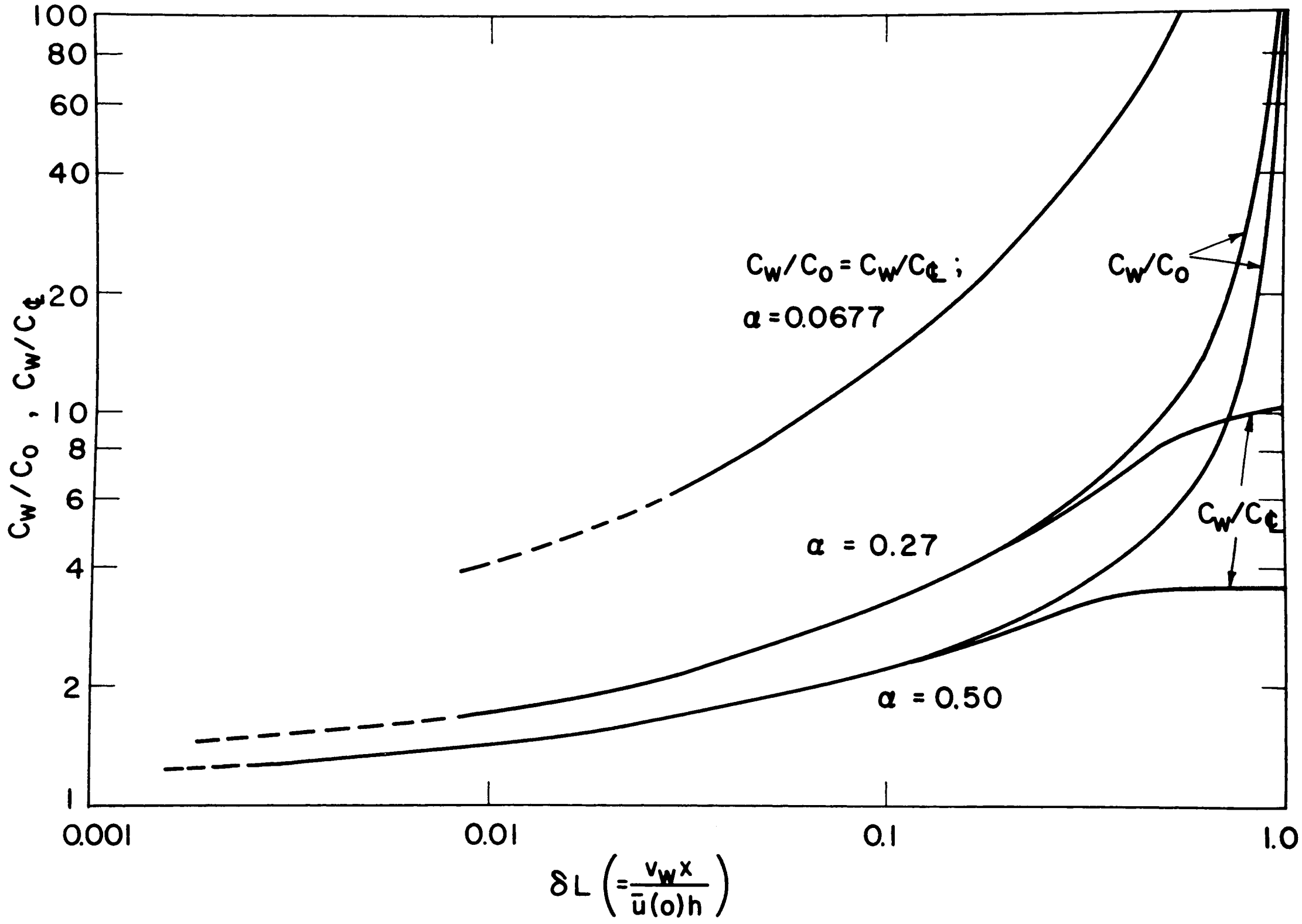

FIGURE 7 VARIATION OF THE SALT CONCENTRATION AT THE WALL WITH α AND δL

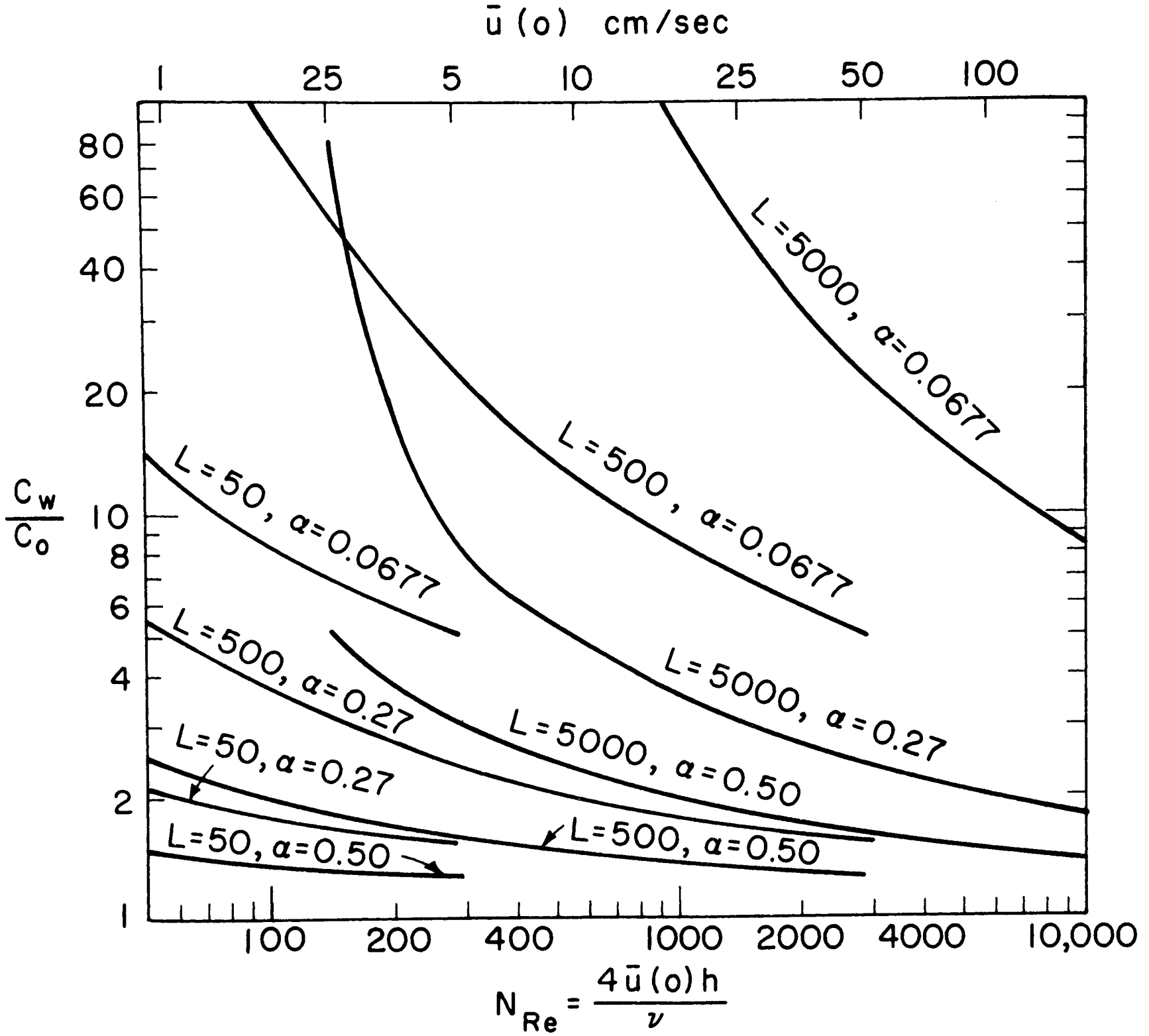
ū (o) cm/sec
1
25
5
10
25
50
100
80
60
40
20
10
8
6
4
2
1
$\frac{C_w}{C_o}$
L=50, α=0.0677
L=500, α=0.0677
L=5000, α=0.0677
L=500, α=0.27
L=5000, α=0.27
L=50, α=0.27
L=5000, α=0.50
L=50, α=0.50
L=500, α=0.50
100
200
400
1000
2000
4000
10,000
$N_{Re} = \frac{4\bar{u}(o)h}{\nu}$

FIGURE 8

Discussion

In order to understand the meaning of the results obtained, it is helpful to consider specific numerical examples. For this purpose ν will be taken as 0.0090 cm^2/sec and D_s as 1.61×10^{-5} cm^2/sec, as in Section 3. Further, assume the channel width to be 0.10 in. (h = 0.127 cm). Then the water flux is proportional to α, as shown below:

α	0.0677	0.27	0.50
v_w cm/sec	18.8×10^{-4}	4.7×10^{-4}	2.54×10^{-4}
v_w gal/(day)(ft^2)	40	10	5.4

This relates the three values of α employed to the water flux in common units.

The parameter $L = \frac{x}{h}$ is the ratio of the channel length to its half-width. For h = 0.127 cm, the values of L of 5,000, 500, and 50 correspond to channel lengths of 635, 63.5, and 6.35 cm, respectively (250, 25, 2.5 in.). The Reynolds number employed as an abscissa in Figure 8 is 56.4 $\bar{u}(o)$, where the average inlet flow velocity $\bar{u}(o)$ is expressed in cm/sec.

As an example, suppose it be stipulated that the salt concentration at the wall must not exceed twice the salt concentration of the feed. Assume that sea water is being supplied to the 0.1 in. channel between two osmotic membranes. Then since osmotic pressure is approximately proportional to salt concentration,

the effective osmotic pressure at the channel outlet will be about twice the normal value, or 760 psia. The minimum feed velocities are obtained directly from Figure 8 by reading N_{Re} at an ordinate of 2, and converting N_{Re}, α, and L to $\bar{u}(o)$, v_w, and x:

Minimum Feed Velocities for $c_w/c_o \leq 2$

v_w, gal/(day)(ft^2)	5.4	5.4	5.4
x, in.	250	25	2.5
$\bar{u}(o)$, cm/sec	17.7	1.77	(0.2)
v_w, gal/(day)(ft^2)	10	10	10
x, in.	250	25	2.5
$\bar{u}(o)$, cm/sec	104	10.4	1.04
v_w, gal/(day)(ft^2)	40	40	40
x, in.	250	25	2.5
$\bar{u}(o)$, cm/sec (estimated)	(15700)	(1570)	(157)

Velocities greater than 100 cm/sec in a 0.1 in. channel would appear to be impractical. This value need not be exceeded if the water withdrawal rate is 10 gal/(day)(ft^2), even if the channel length is 20 ft. The situation worsens rapidly, however, as the water withdrawal rate is increased. At 40 gal/(day)(ft^2) the channel length is limited to about 1.6 in. at a flow

velocity of 100 cm/sec.

Another way of visualizing the results is to employ Figure 8 to estimate c_w/c_o for a feed velocity of 30.5 cm/sec (1.0 ft/sec). This corresponds to N_{Re} = 1720.

Salt Build-Up at a Flow Rate of 30.5 cm/sec

v_w, gal/(day)(ft^2)	5.4	5.4	5.4
x, in.	250	25	2.5
c_w/c_o	1.75	1.3	(1.2)
v_w, gal/(day)(ft^2)	10	10	10
x, in.	250	25	2.5
c_w/c_o	2.9	1.73	1.3
v_w, gal/(day)(ft^2)	40	40	40
x, in.	250	25	2.5
c_w/c_o	39	6.4	3.1

The indication again is that salt build-up becomes very serious at the larger water withdrawal rates, even for quite short channels.

The values of c_w/c_o obtained refer to conditions at the channel outlet: for the channel as a whole the average value of this ratio is roughly that at x/2, which is considerably greater than half that at the duct outlet. Since c_w increases along the

flow direction, the water withdrawal rate will decrease as c_w and the effective osmotic pressure increase. The extent of the variation in v_w will depend largely on the amount by which the total pressure exceeds the effective osmotic pressure at the outlet. though the analysis does not allow for this variation of v_w with x, the meaning of the calculated curves is clear.

The effects in laminar flow are more complicated than in the turbulent flow cases considered in Section 3, but the general conclusions are the same for both regimes. Salt build-up is serious even with the modest water fluxes attainable with present-day membranes employed for reverse osmosis. As better membranes are produced, permitting appreciably greater water production the salt build-up effect will become more and more important. Sophisticated equipment designs, perhaps employing boundary layer withdrawal, will be required if excessively high operating total pressures are to be avoided.

6. Laminar Flow in a Round Tube

Mahon (8) has described the use of membranes in the form of small tubes, and it would be of interest to investigate the importance of salt build-up at the walls of a tubular osmotic membrane.

The analytical problem is similar to that of the two-dimensional duct. The velocity field has been described by Yuan and Finkelstein (16), and the analysis would be expected to proceed

in a fashion analogous to that employed for the two-dimensional duct in Section 5.

One might speculate that the ratios c_w/c_o would be somewhat smaller for the round tube than for the duct at the same brine velocity, since the ratio of membrane surface to channel volume is greater.

7. Salt Precipitation

Throughout this report, emphasis has been placed on the influence of salt build-up at a membrane surface on the effective osmotic pressure which must be overcome to give a positive water flux through the membrane. The problem of calcium sulfate or other salt precipitation can evidently be treated by use of the analysis and graphs presented. Thus if the solubility of calcium sulfate is three times the concentration of calcium sulfate in the brine, precipitation at the membrane surface may be anticipated if c_w/c_o reaches 3. Conditions under which this will occur may be derived from the analysis presented, where c_w and c_o pertain to the salt in question, and D_s represents the diffusion coefficient of this salt in brine. Salt precipitation at the membrane surface may sometimes prove to be even more serious than the required increase in operating pressure.

Acknowledgment

The machine computations presented here were performed at the Massachusetts Institute of Technology Computation Center. The authors are grateful for the use of its facilities.

Appendix

Table 1 - Eigenvalues and the Constants of Equation 52
for $\alpha = 0.50$, 0.27 and 0.0677

	β_n			B_n		
n	$\alpha = 0.50$	$\alpha = 0.27$	$\alpha = 0.0677$	$\alpha = 0.50$	$\alpha = 0.27$	$\alpha = 0.0677$
1	0.00000000	0.00000000	0.00000000	0.72358631	0.50564340	0.00722845
2	8.1246586	4.0993398	1.5260594	0.32545579	0.55726079	0.99915998
3	33.039892	17.455850	5.3774762	-0.06900341	-0.08699855	-0.00936713
4	74.049603	39.500552	10.955489	0.03095925	0.03709633	0.00479673
5	131.11500	70.225842	18.612657	-0.01783755	-0.02090765	-0.00293043
6	204.21702	109.61998	28.424291	0.01169970	0.01353716	0.00195953
7	293.34489	157.67553	40.404236	-0.00831358	-0.00953389	0.00139714
8	398.50960	214.38200	54.555180	0.00622361	0.00711175	0.00104494
9			70.877450			-0.00081074

Table 2 - Values of the Radial Eigenfunctions

n	R = 0.0	0.1	0.2	0.3	0.4	0.5	0.6	0.7	0.8	0.9	1.0
						α = 0.0677					
1	1.0000000	1.1169460	1.5529824	2.6700310	5.6139719	14.213225	42.473999	146.21004	563.30752	2349.6026	10217.993*
2	1.0000000	.99800619	.99109353	.97553844	.94061152	.85389311	.60712733	- .19986140	- 3.1806780	- 15.262847	- 67.117304
3	1.0000000	.71719532	- .08853417	-1.2895360	-2.6703436	-3.9030535	-4.4345902	- 3.0301552	4.1071753	31.557337	142.77626
4	1.0000000	.35707563	- .96400767	-1.5322086	- .05942415	3.5666601	7.6648905	8.5420639	- .73935486	- 38.991583	- 184.02736
5	1.0000000	-.05496837	-1.2607338	.10193418	2.5229737	.93172398	-6.5571339	-13.300827	- 5.2596299	40.490275	202.96085
6	1.0000000	-.45953395	- .81400080	1.5927170	.11011703	-4.1005276	1.2253064	15.040547	12.334374	- 39.140844	- 212.80680
7	1.0000000	-.79344013	.11517963	1.1113050	-2.4929088	1.9172768	4.8455174	-12.697252	-19.345878	36.169671	218.73829
8	1.0000000	-1.0038061	.97539808	- .74360780	- .16958188	2.7451731	-7.4064191	6.6479542	25.336821	- 32.085717	- 222.76142
9	1.0000000	-1.0570969	1.2531976	-1.6734601	2.4792107	-3.7842900	4.6158551	1.4083348	-29.510443	27.148490	225.74820
						α = 0.27					
1	1.0000000	1.0281195	1.1166915	1.2792193	1.5412481	1.9454810	2.5599813	3.4901813	4.8946762	7.0023792	10.123048*
2	1.0000000	.95188390	.80773134	.56779981	.23134009	- .20547661	- .75317039	- 1.4350734	- 2.2976524	- 3.4279104	- 4.9826000
3	1.0000000	.71662536	.00235583	- .79957204	-1.2973468	-1.2210158	- .51963516	.65722521	2.0777752	3.5942351	5.3184113
4	1.0000000	.37018920	- .77560792	-1.0664733	- .06151542	1.2797190	1.6165446	.47386815	- 1.5534886	- 3.6082769	- 5.5012238
5	1.0000000	-.03269836	-1.0665769	.03476070	1.2967642	.26811357	-1.6398150	- 1.5345585	.83086084	3.5469307	5.6432933
6	1.0000000	-.4284087	- .70491578	1.088619	.05080174	-1.4752544	.50284304	2.1481407	.00672914	- 3.4239269	- 5.7639780
7	1.0000000	-.75492346	.08393543	.77187106	-1.2959977	.76663797	1.0019535	- 2.0872540	- .86833660	3.2454434	5.8703762
8	1.0000000	-.96083915	.82094488	- .51223222	- .06497280	.94512064	-1.7815840	1.3511912	1.6615406	- 3.0154228	- 5.9664022
						α = 0.50					
1	1.0000000	1.0150877	1.0614119	1.1422214	1.2631391	1.4324338	1.6612992	1.9639838	2.3574958	2.8604386	3.4903429*
2	1.0000000	.93426133	.74301243	.44321394	.06011353	- .37690628	- .83947622	- 1.3059283	- 1.7672322	- 2.2332758	- 2.7402792
3	1.0000000	.69980481	- .03311978	- .79445356	-1.1735293	- .96707484	- .25194367	.70447329	1.6177535	2.3373167	2.9176569
4	1.0000000	.35579205	- .77407790	- .98919151	.00781126	1.1394716	1.2383615	.18209732	- 1.2642854	- 2.3675517	- 3.0414313
5	1.0000000	-.04318372	-1.0383163	.06856717	1.1737917	.15683228	-1.3557762	- 1.0410653	.76113642	2.3469994	3.1406060
6	1.0000000	-.43417685	- .67246751	1.0387626	.00062783	-1.2516761	.48814960	1.5749042	- .16607074	- 2.2832885	- 3.2244334
7	1.0000000	-.75566733	.09909869	.70830666	-1.1738443	.70536433	.74055590	- 1.5954227	- .45590233	2.1808731	.32975307
8	1.0000000	-.95720032	.81044245	- .50671679	- .02169716	.76968649	-1.4257174	1.0882428	1.0369185	- 2.0439389	- 3.3623333

* Shown are the values calculated from the infinite series. The agreement with the analytical expression (Equation 64) is good.

References

(1) Berman, A. S., J. Appl. Phys. 24, 1232 (1953).

(2) Deissler, R. G., NACA Rept. 1210 (1955).

(3) Drew, T. B., E. C. Koo, and W. H. McAdams, Trans. Amer. Inst. Chem. Engrs., 28, 56 (1933).

(4) Eisenberg, M., C. W. Tobias, and C. R. Wilke, Chem. Eng. Progr. Symp. Ser. 51, No. 16, 1 (1955).

(5) Hildebrand, F. B., "Advanced Calculus for Engineers", pp. 132-147. Prentice-Hall, Inc., Englewood Cliffs, N.J. 1949.

(6) Hildebrand, F. B., ibid., pp. 224-232.

(7) Loeb, S., and S. Manjikian, U.C.L.A. Report 63-22, May 1963.

(8) Mahon, H. I., Proc. Desalination Research Conference, p. 345. National Academy of Sciences, Publ. 942 (1963).

(9) Merten, U., H. K. Lonsdale, and R. L. Riley, paper presented at the Los Angeles meeting of the Amer. Chem. Soc., April 4, 1963.

(10) Merten, U., H. K. Lonsdale, and J. C. Westmoreland, General Atomics Corp. Report GA-3962, February 28, 1963.

(11) Sherwood, T. K., and R. L. Pigford, "Absorption and Extraction", 2nd ed. 1952. McGraw-Hill Book Co., New York.

(12) Sherwood, T. K., Chem. Eng. Progr., Symp. Ser. 55, No. 25, 71, (1959).

(13) Sherwood, T. K., and J. M. Ryan, Chem. Eng. Sci., 11, 81 (1959).

(14) Theodorsen, T., and A. Regier, NACA Tech. Rept. 793 (1944).

(15) Vieth, W. R., J. H. Porter, and T. K. Sherwood, I&EC Fundamentals 35, 1 (1963).

(16) Yuan, S. W., and A. B. Finkelstein, Trans. A.S.M.E., 78, 719 (1956).

Table of Nomenclature

c = solute (salt) concentration, g moles/cm^3.

c_L = water concentration in solution, g moles/cm^3.

c_o = solute (salt) concentration in bulk or feed solution, g moles/cm^3.

c_w = solute (salt) concentration at phase boundary, g moles/cm^3.

C = c/c_o.

d = diameter, cm.

D_s = molecular diffusion coefficient, salt in solution, cm^2/sec.

f = Fanning friction factor.

$f(L)$ = $\frac{3}{2}$ $(1 - \delta L)$.

F = water flux across phase boundary, g moles/(sec)(cm^2).

$g(R)$ = $1 - R^2$.

h = half-width of two-dimensional channel, cm.

j_D = dimensionless group defined by Equation 4.

k_s^o = mass transfer coefficient, cm/sec.

L = x/h.

N_F = water withdrawal flux parameter, = $\frac{v_w h}{\nu}$.

N_{Re} = Reynolds number based on channel diameter or width.

N_{Sc} = Schmidt number, ν/D_s.

p = pressure, g/cm^2.

R = y/h.

u = velocity component in x-direction, cm/sec.

u_o = bulk fluid velocity, cm/sec.

$u^+ = \frac{u}{u_o}\sqrt{\frac{2}{f}}$.

$\bar{u}(o)$ = average fluid velocity at duct entrance, cm/sec.

$U = u/\bar{u}(o)$.

v = velocity component in y-direction, cm/sec.

v_w = water withdrawal flux, cm/sec.

$V = v/v_w$.

x = distance in direction of bulk fluid flow, cm.

X = solution of the axial eigenfunction.

y = distance in direction normal to phase boundary, cm.

y_1 = film thickness, cm.

$y^+ = \frac{u_o y}{\nu}\sqrt{\frac{f}{2}}$.

$y^{++} = y^+\sqrt{f/2}$.

Y = solution of the radial (or transverse)eigenfunction

$\alpha = D_s/v_w h$.

$\delta = v_w/\bar{u}(o)$.

ϵ = eddy diffusion coefficient, cm^2/sec.

ν = kinematic viscosity, cm^2/sec.

ρ = fluid density, g/cm^3.

USCOMM-DC-51858